Journal of Applied Polymer Science

Hydrolytic degradation of nanocomposites based on poly(L-lactic acid) and layered double hydroxides modified with a model drug

Andrea Oyarzabal,[1] Agurtzane Mugica,[1] Alejandro J Müller,[1,2] Manuela Zubitur[1,3]

[1]POLYMAT and Polymer Science and Technology Department, Faculty of Chemistry, University of the Basque Country UPV/EHU, Paseo Manuel De Lardizabal 3, 20018, Donostia-San Sebastián, Spain

[2]IKERBASQUE, Basque Foundation for Science, Bilbao, Spain

[3]Chemical and Environmental Engineering Department, Polytechnic College of Donostia, University of the Basque Country UPV/EHU, Plaza De Europa 1, 20080, Donostia-San Sebastián, Spain

Correspondence to: M. Zubitur (E-mail: manuela.zubitur@ehu.eus)

ABSTRACT: Hydrolytic degradation of a nanocomposite of poly(L-lactic acid), PLA, and a layered double hydroxide (LDH) modified with the drug 4-biphenyl acetic acid (Bph) has been studied. PLA/LDH-Bph nanocomposite was prepared by solvent casting with 5 wt % of drug modified LDH and the hydrolytic degradation was carried out in a PBS solution at pH 7.2 and 37 °C. Neat PLA with 5 wt % 4-biphenyl acetic acid was studied as reference material (PLA/Bph). The materials were studied by WAXS, TEM, TGA, DSC, SEM, FTIR, SEC and contact angle measurements. For PLA/Bph, an acid catalytic effect, caused by the drug, accelerates PLA mass loss. However, for PLA/LDH-Bph, the presence of LDH produces a barrier effect that initially reduces the diffusion of the oligomers produced during hydrolytic degradation. DSC results demonstrate that Bph induces faster PLA crystallization and this effect is reduced in PLA/LDH-Bph nanocomposites because of their lower drug content. © 2016 Wiley Periodicals, Inc. J. Appl. Polym. Sci. **2016**, *133*, 43648.

KEYWORDS: clay; degradation; polyesters

Received 11 January 2016; accepted 16 March 2016
DOI: 10.1002/app.43648

INTRODUCTION

Poly(L-lactide) (PLA) is a biodegradable and biocompatible aliphatic polyester that is widely used in biomedical applications,[1] such as drug delivery systems,[2] bone fixation devices[3] and implants.[4] However, neat PLA has limited applications as a consequence of its relatively poor mechanical properties, slow crystallization rate, and slow degradation rate. In order to overcome these disadvantages, copolymerization,[5] stereocomplexation[6] and polymer blending methods have been employed.[7]

In addition, the preparation of polymer/clay nanocomposites are an alternative to improve the properties of PLA, even at very low nanofiller contents, as a consequence of the enhanced interfacial area provided by the dispersion of nanoclay layers in the polymer matrix.[8,9] Improvements in properties broaden the end-use properties of PLA including mechanical, thermal, gas barrier and flame-retardant properties.[10]

Polymer/clay nanocomposites based on biodegradable polymers can also be used in biomedical devices for controlled release of therapeutic agents. A large number of researchers have examined the effect of the presence of layered nanocomposites in drug containing biopolymer matrixes.[11–13] It has been found, that the tortuous path of drug diffusion produced by the clay layers can tailor drug release.

An interesting approach is the use of layered double hydroxides (LDH), also known as anionic clays, as nanofillers in bionanocomposites for controlled release vehicles. The structures of LDHs consist of brucite-like sheets, in which divalent cations are partially replaced by trivalent cations, and interlayer anions compensate for the positively charged layers.[14]

The general formula for LDH materials is $[M^{2+}_{1-x}M^{3+}_{x}(OH)_2]^{x+}(A^{n-})_{x/n}.mH_2O$, where M^{2+} and M^{3+} are the individual divalent and trivalent cations in octahedral sites within the OH^- layers. A^{n-} is an exchangeable anion such as CO_3^{2-} or NO_3^-. In general, LDHs can be prepared by several methods with high purity.[15] They are economic, biocompatible, and can be organically modified with a variety of organic anions, of which there are many more available than organic cations. LDHs have been modified with several bioactive substances, such as: anti-inflammatories,[16] antibiotics,[17] and herbicides.[18]

Additional Supporting Information may be found in the online version of this article.

Tammaro *et al.* prepared nanocomposite films of PCL and LDH modified with an antifibrinolytic drug or with antibiotics.[19,20] They concluded that the presence of LDH allows tailoring drug release by modifying factors like ionic force of the surrounding solution, concentration of the drug inside the inorganic lamellae, concentration of the inorganic component into the polymeric matrix, thickness and shape of the sample.

The properties and drug release of nanocomposites based on PLA or copolymers with LDH modified with drugs have also been studied. Dagnon *et al.*[21] prepared PLA nanocomposites with LDH functionalized with ibuprofen and they obtained a decrease in cell adhesion and an increase in mechanical performance of the films.

Chakraboti *et al.*[22] studied the potential of nanocomposite films based on poly(lactide-co-glycolic acid) with LDH containing antibiotics as systems to treat disease states that require drug exposure for long time.

Miao *et al.*[23] found a different behavior in drug release using electrospun fibers of layered double hydroxide nanocomposites based on PCL or PLA. In the case of PCL nanocomposites with drug modified LDH, the release is slower compared with a system in which the drug is dispersed in the polymer matrix. However, the release is faster in the PLA-based system, probably due to the interaction between drug and PLA.

More recently, San Román *et al.*[24] studied drug release from PLA nanocomposites with LDH intercalated with different drugs. They found that drug release is slower when LDHs are dispersed in PLA as a consequence of the slow degradation of this polymer.

Understanding PLA hydrolytic degradation mechanism is important to design and develop controlled drug release PLA based materials.[25] Its hydrolytic degradation takes place in the bulk of the material rather than at its surface and it proceeds through hydrolysis of the ester linkage, while the carboxylic acid produced catalyzes the degradation reaction.[26] The hydrolytic degradation mechanisms can be affected by various factors, such as crystallinity degree, morphology, molecular weight and its distribution, as well as the conditions under which hydrolysis is conducted (temperature and pH).[27,28] In addition, it has been found that certain type of drugs may exert a catalytic effect on PLA hydrolytic degradation.[29,30]

The addition of nanoclays can significantly alter the hydrolysis degradation behavior of PLA. Conflicting results on their effect can be found in the literature.

Several authors found an accelerating effect of nanoclays on hydrolytic degradation of PLA as a consequence of the hydrophilicity of the clay layers.[31–33] Zhou and Xhantos[34] concluded that polymer degradation starts at the interface between polymer matrix and fillers and that the degree of dispersion enhances hydrolytic degradation.

However, other authors reported that nanoclays retarded the degradation of PLA because they induced its crystallization.[35] Roy *et al.*[36] observed a change in the pattern of the degradation products in presence of nanoclays, suggesting that longer oligomers could be partially trapped by the clay layers leading to a catalytic effect. This effect results in higher mass loss at later stages of hydrolysis in PLA/clay nanocomposites as compared to neat PLA. Therefore, it can be concluded that the hydrolysis of PLA in the presence of nanofillers is a complex phenomenon that depends on the nature and dispersion of nanoclay and polymer crystallinity. In this context, the thermal properties of nanocomposites based on LDHs and biodegradable polymer matrices have already been studied.[9,37,38] However, little work has been done on the effect of the presence of LDH on the hydrolytic degradation of PLA nanocomposites. Zhou and Xhantos[39] studied the effect of unmodified LDH on the hydrolytic degradation of polylactides. They found a reduction in degradation rate, probably due to the reduction of the carboxylic group catalytic effect through neutralization with the basic LDH surface. Moreover, more knowledge is needed in order to elucidate the complex interactions between PLA and LDH/drug combinations in controlled release systems.

In this work, nanocomposites of PLA with LDH modified with a drug (biphenyl acetic acid) that is a potent non-steroidal anti-inflammatory agent used to treat muscle inflammation and arthritis, were prepared.[40] The aim is to investigate the effects of the drug modified LDH on PLA hydrolytic degradation behavior. Neat PLA filled with biphenyl acetic acid has been also studied as a reference material.

EXPERIMENTAL

Materials

The PLA used in this work is a commercial grade (3052D) purchased from Natureworks (4 wt % D-lactide content). PLA pellets were purified by dissolution in tetrahydrofuran (THF) and subsequent precipitation in an excess of methanol. The precipitated PLA was filtered and dried in vacuum at 60 °C for 48 h. Hydrotalcite [$Mg_6Al_2(OH)_{16}CO_3$] (LDH) was supplied by Wako Pure Chemicals Industries Ltd (AEC =350 meq/100 g). 4-biphenyl acetic acid (Bph) was obtained from Aldrich and used without further purification. THF and methanol were used as received.

Modification of LDH

The LDH interlayer anions have been intercalated by the restacking method, in which calcinated LDH (6 h at 500 °C) is added to a solution of biphenyl acetic acid in deionized water (the pH of the solution was adjusted to 10 by NaOH addition). The solution reaction was then refluxed under stirring and a nitrogen atmosphere for 7 h. The obtained solid was separated by centrifugation, suspended in decarbonated water, and centrifuged several times. The organomodified LDH (LDH/Bph) was dried under vacuum at 60 °C during 48 h.

Preparation of Nanocomposites

Polymer films were prepared by solvent casting. Concentrations used varied depending on the system: 1.5 g PLA/50 mL THF for PLA films, 1.5 g PLA/40 mL THF and 0.075 g biphenyl acetic acid/10 mL THF for PLA/Bph films.

In the case of PLA/LDH-Bph films 1.5 g of PLA were dissolved in 40 mL THF. Simultaneously, 0.075 g of dried LDH (at 60 °C under vacuum for 24) were dispersed in 10 mL THF and stirred

with sonication during 2 h. Subsequently, the PLA solution and the LDH dispersion or drug dissolution were mixed together and stirred with sonication for 3 h. Films were formed by subsequent solution-casting in Petri dishes. The solvent was allowed to evaporate gently in order to avoid bubble formation. The resulting polymer films were dried under vacuum at room temperature until constant weight was obtained. For brevity, the film containing 5 wt % of 4-biphenyl acetic acid is abbreviated as PLA/Bph and the film containing 5 wt % LDH/Bph is abbreviated as PLA/LDH-Bph.

Hydrolytic Degradation

The films prepared by casting were cut into small pieces (1 cm × 1 cm × 200 μm), weighed and placed in vials containing 10 mL of phosphate buffered saline solution (PBS, pH 7.2). The vials were left in a circulating water bath at 37 °C. After the required incubation time (14, 21, 28, 35, 42 and 56 days) the specimens were removed, washed in distilled water, and vacuum dried until constant weight was achieved at room temperature prior to characterization. The pH of the ageing media was monitored once a week using a pH meter (MP120, Mettler-Toledo, Switzerland).

The remaining degradation media was analyzed by Ultraviolet-visible (UV–vis) spectroscopy for biphenyl acetic acid concentration at a wavelength of 252 nm. The spectra were recorded in a Jenway 7305 Spectrophotometer. The measurements were performed in duplicate and the mean value was calculated.

Weight loss during film degradation was measured by the changes in dry weight after incubation in PBS (pH 7.2) at 37 °C. At preset time intervals (14, 21, 28, 35, 42 and 56 days), hydrated films were weighed after they were wiped with soft paper tissue to remove surface water. Values obtained for duplicate samples were averaged. Percentage weight loss was calculated according to the following equation:

$$\%\text{Weight loss} = 100 \times \frac{W_0 - W_t}{W_0} \quad (1)$$

where W_0 is the starting film weight, W_t is the film weight at time, t.

X-ray Diffraction

X-ray diffraction patterns were recorded in a Philips PW 1729 GXRD X-ray diffractometer at 45 kV and 50 mA, using Ni-filtered Cu Kα radiation source over a 2θ range of 1–60°, with a step size of 0.05° and a counting time of 5 seconds per step.

Fourier Transformed Infrared Spectroscopy

The FTIR spectra were recorded using a Nicolet MAGNA-IR 560 Spectrometer and KBr disks. Infrared Spectra were collected at a resolution of 2 cm^{-1} and a minimum of 64 scans were signal averaged in the 400-4000 cm^{-1} range.

Transmission Electron Microscopy

Bright-field TEM images of the nanocomposites were obtained at 200 kV with a Philips Tecnai 20 apparatus. The samples were ultrathin-sectioned at ~40 nm using a cryogenic ultramicrotome.

Scanning Electron Microscopy

Sample surface morphology before and after the degradation was observed by scanning electron microscope (SEM) after gold-coating using a Hitachi S-2700 electron microscope operated at an accelerating voltage of 15 kV.

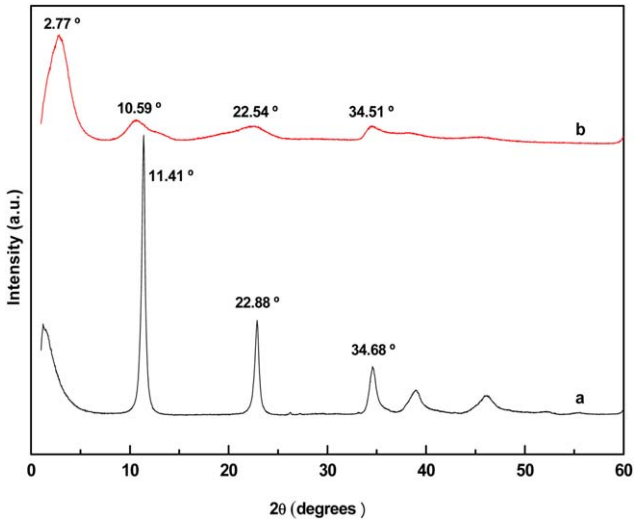

Figure 1. XRD patterns of (a) LDH, (b) LDH organically modified with Bph (LDH-Bph). [Color figure can be viewed in the online issue, which is available at wileyonlinelibrary.com.]

Thermal Properties

Thermal properties were determined by Differential Scanning Calorimetry using samples of approximately 5 mg that were encapsulated in aluminium pans and measured in a Perkin Elmer PYRIS 1 DSC calibrated with indium and dodecane, under ultrapure nitrogen atmosphere. All samples were heated from 0 °C to 200 °C at 10 °C min^{-1} and kept for 3 min at 200 °C to erase thermal history. Then, the samples were cooled to 0 °C at 10 °C min^{-1}, hold for 1 min at 0 °C and finally, the samples were heated from 0 °C to 200 °C at the same rate. Both heating scans were recorded.

Contact Angle Measurement

Wettability was evaluated by contact angle measurements that were performed in an OCA20 instrument at static mode (Sessile drop) at 25 °C at 55% of relative humidity. Measurement of a given contact angle was carried out for at least 5 times. Milli-Q water (10 μL) was used as probe liquid.

Size Exclusion Chromatography

Size exclusion chromatography (SEC) measurements were performed on a Waters apparatus with refractive index detector. THF was used as mobile phase at a flow rate of 1.0 mL min^{-1}. Calibration was accomplished with polystyrene standards. The samples were prepared by dissolving ≈10 mg of sample into 5 mL of THF and then the solution was filtered by means of a Nylon Scharlau 0.45 μm filter.

RESULTS AND DISCUSSION

Characterization of Modified LDH

The confirmation of the intercalation of the drug (4-biphenyl acetic acid) into the clay gallery was carried out by XRD analysis. Figure 1 shows the XRD patterns of neat LDH and modified LDH with 4-biphenyl acetic acid (LDH-Bph). Neat LDH shows three strong diffraction peaks at $2\theta = 11.41$, 22.88, and 34.68°,

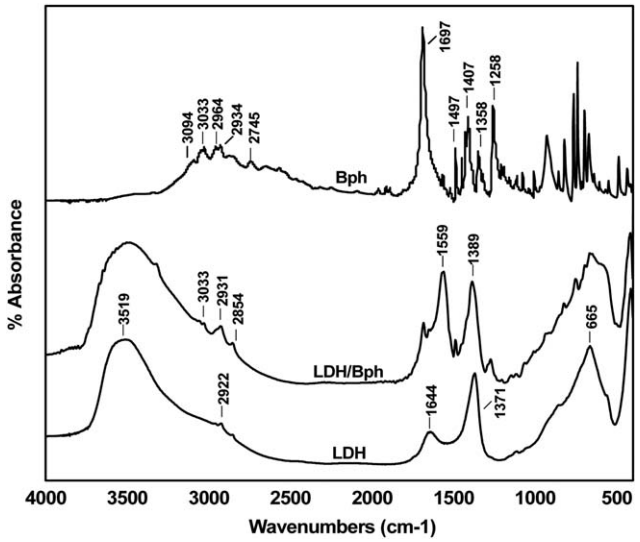

Figure 2. FTIR spectra of LDH, Bph and LDH organically modified with Bph (LDH-Bph).

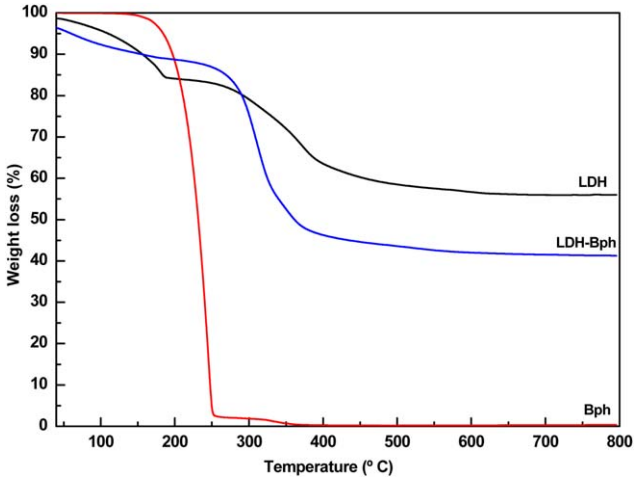

Figure 3. TGA curves for (a) LDH, (b) 4-biphenyl acetic acid and (c) LDH-Bph obtained in N_2 atmosphere. [Color figure can be viewed in the online issue, which is available at wileyonlinelibrary.com.]

corresponding to (003), (006) and (009) basal reflections. Upon the incorporation of the drug the interlayer distance of LDH increases from 0.77 nm to 3.19 nm (corresponding to a change in 2θ values from 11.41° to 2.77°).

Molecular dimensions of 4-biphenyl acetic acid were determined based on its three-dimensional (3D) structure by taking the lengths of the edges of a box encompassing the molecules. The dimensions thus calculated reflect the molecular length, molecular width and molecular thickness. The molecular visualization software "Jmol" was used for this purpose.[41] The calculated dimensions for 4-biphenyl acetic acid were 1.20 × 0.36 × 0.42 nm. As the increase in interlayer distance (2.42 nm) is much larger than the molecular length of biphenyl acetic acid, it is suggested that the drug molecules are arranged as a partially inter-digitated bilayer. Khan *et al.*[42] modified a Li-Al layered double hydroxide with 4-biphenyl acetic acid and they also found a bilayer arrangement with an interlayer distance of 2.04 nm. In summary, the results are consistent with the inclusion of 4-biphenyl acetate anions in the interlayer of LDH.

The XRD pattern of LDH-Bph in Figure 1 also shows a weak peak at 10.59° that can indicate the presence of a small amount of interlayer CO_3^{2-}.

The FTIR spectra of 4-biphenyl acetic acid, neat LDH and LDH modified with the drug are shown in Figure 2. Neat LDH exhibits the following bands: stretching of the OH groups of the layer at 3519 cm^{-1}, stretching vibrations of carbonate ions at 2922 cm^{-1}, bending mode band of interlayer water molecules at 1644 cm^{-1}, carbonate stretching mode at 1371 cm^{-1} and finally, the peak at 655 cm^{-1} is assigned to the metal-oxygen modes of the LDH sheets.[43]

Figure 2 also shows bands corresponding to 4-biphenyl acetic acid: the characteristic C=O stretching vibrations at 1697 cm^{-1} (carboxylic acid), a band around 1560-1400 cm^{-1} assigned to ring vibrations and ν(CH) vibrations at 3100-2500 cm^{-1}. As the restacking has been carried out at high pH, LDH-Bph shows peaks corresponding to symmetric and asymmetric modes of COO^- at 1389 and 1559 cm^{-1}, respectively. The presence of these bands confirms the intercalation of the drug within LDH. The complete disappearance of carbonate ions cannot be confirmed because the characteristic band may be overlapped with the COO^- symmetric stretching band.

TGA curves of LDH, 4-biphenyl acetic acid and LDH-Bph are shown in Figure 3. Neat LDH shows step wise weight losses at 50–200 °C (loss of surface and interlayer water), 250–500 °C (dehydroxilation/decomposition of interlayer carbonate anions) and 500–800 °C, corresponding to the dehydroxilation/decomposition of interlayer carbonate anions.[44]

The LDH-Bph first exhibits a weight loss up to 150 °C, corresponding to the amount of interlayer water that leaves the sample, see Figure 3. The weight loss from 200 to 350 °C is due to the decomposition of anions in 4-biphenyl acetate and within the layered double hydroxide host.

The drug content in LDH-Bph is 24% determined by UV-vis spectroscopy by measuring the drug released after 5 days of incubation in PBS buffer.

Morphology of PLA Nanocomposite

The morphology of PLA nanocomposites was analyzed by XRD and TEM. Figure 4 shows XRD patterns of pure PLA, PLA with Bph and PLA/LDH-Bph. As can be seen in the inset, for PLA/LDH-Bph no peaks corresponding to LDH-Bph are observed and this is probably due to exfoliation or to the presence of disordered LDH layers.

XRD alone cannot characterize the morphology of nanocomposites with clay nanofillers with layer structures, since it cannot detect layers that are not in parallel registry. Figure 5 shows TEM images of PLA/LDH-Bph at low (left) and high (right) magnifications. The dispersion of modified LDH is good, as demonstrated by the image at low magnification that shows small tactoids. Evidence of the formation of a nanocomposite with a partially exfoliated morphology is shown in the TEM

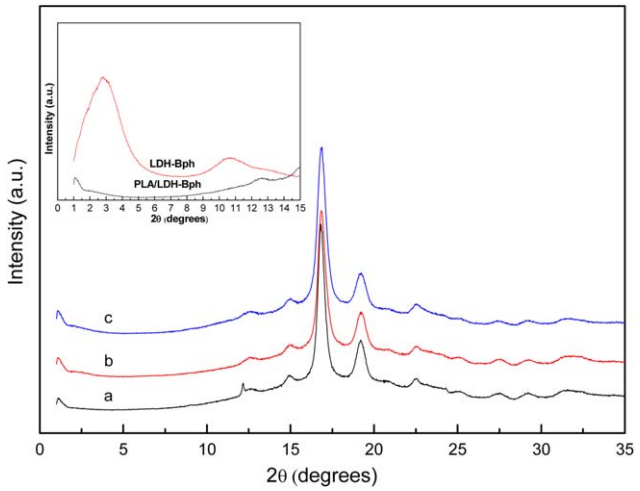

Figure 4. XRD patterns of (a) neat PLA, (b) PLA/Bph and (c) PLA/LDH-Bph films. The inset shows the XRD pattern of LDH-Bph and PLA/LDH from 1 to 15°. [Color figure can be viewed in the online issue, which is available at wileyonlinelibrary.com.]

image at higher magnification in which some exfoliated clay layers can be observed as black lines. These results corroborate the results obtained by XRD where no peaks corresponding to LDH-Bph were observed.

Mass Loss and Hydrophobicity

Figure 6(I) shows the total weight loss curves for PLA, PLA/Bph and PLA/LDH-Bph measured at different incubation times. An increase in weight loss with immersion time can be observed in all cases. Neat PLA exhibits the lowest weight loss with just 6 wt % after 56 days. For neat PLA, this weight loss accounts for water-soluble oligomers formed by hydrolysis and released to the incubation media.

PLA/Bph shows the highest degradation rate indicating that the presence of the drug accelerates mass loss [Figure 6(I)]. It should be taken into account that for PLA/Bph, weight loss could come from the release of both biphenyl acetic acid and water soluble oligomers produced by PLA degradation. For PLA/Bph, Figure 6(I) shows the total weight loss, representing dissolution of all soluble compounds (drug and PLA oligomers).[45] Figure 6(II), on the other hand, shows weight losses due only to polymer degradation (polymer weight loss). Under these conditions, it was observed that after 56 days of degradation PLA lost 21% of its weight in the case of PLA/Bph.

Among the several factors that affect PLA degradation, the degree of crystallinity (X_c) has to be considered.[46] DSC scans of PLA, PLA/Bph and PLA/LDH-Bph corresponding to their first heating scans show that all films have similar crystallinity values of X_c=28%. Therefore, this factor is not responsible for the differences in mass loss observed for neat PLA and PLA/Bph (Figure 6).

The low degradation rate observed in neat PLA could be a consequence of its hydrophobic structure.[32] Hydrophobicity provokes low penetration and diffusion of water into the polymeric matrix. The hydrophilicity of a film can be evaluated by the contact angle of water droplets (Table I). The contact angle of neat PLA is around 84°, similar to the value reported in the literature.[47]

The addition of Bph to PLA does not change its hydrophilicity (Table I), therefore, this is also not the reason for faster weight loss of PLA/Bph as compared to neat PLA.

The acceleration of mass loss in drug loaded PLA is probably due to the effect of acid catalysis produced by biphenyl acetic acid on PLA degradation. Hydrolysis of ester groups within biodegradable polymers can be catalyzed by acids or bases. It has been reported that the presence of acidic drugs lead to a faster hydrolysis of ester bonds, due to acid catalysis.[48] In the case of basic drugs, an acceleration of hydrolytic degradation as consequence of base catalysis of the ester bond hydrolysis has also been observed.[49] However, in some cases a retardation has been measured because the basic drug can neutralize the carboxylic end groups of polymer chains.[50]

The acceleration of polymer degradation by the acidic drug can be confirmed by the optical images of the samples after hydrolysis (see Figure 7). For neat PLA, the visual observations show that the degree of hydrolytic degradation is very small because after 56 days, the sample appears almost invariant. However, PLA/Bph films show integrity loss at 28 days of hydrolysis, as the sample broke in small pieces while degradation proceeded.

For PLA/LDH-Bph, two stages can be observed in the weight loss behavior [Figure 6(II)]. In the first stage, weight loss is lower than for neat PLA indicating a higher resistance to hydrolysis. As can be seen in Table I, the presence of nanoclay reduces

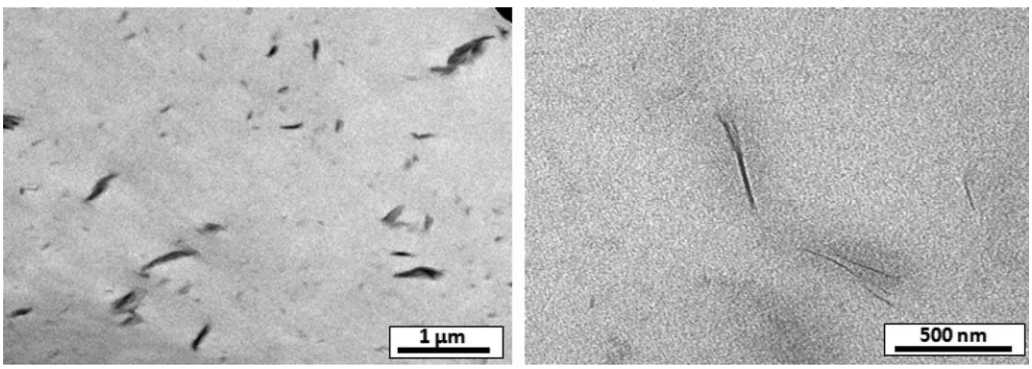

Figure 5. TEM micrographs of PLA/LDH-Bph at low (left) and high (right) magnification.

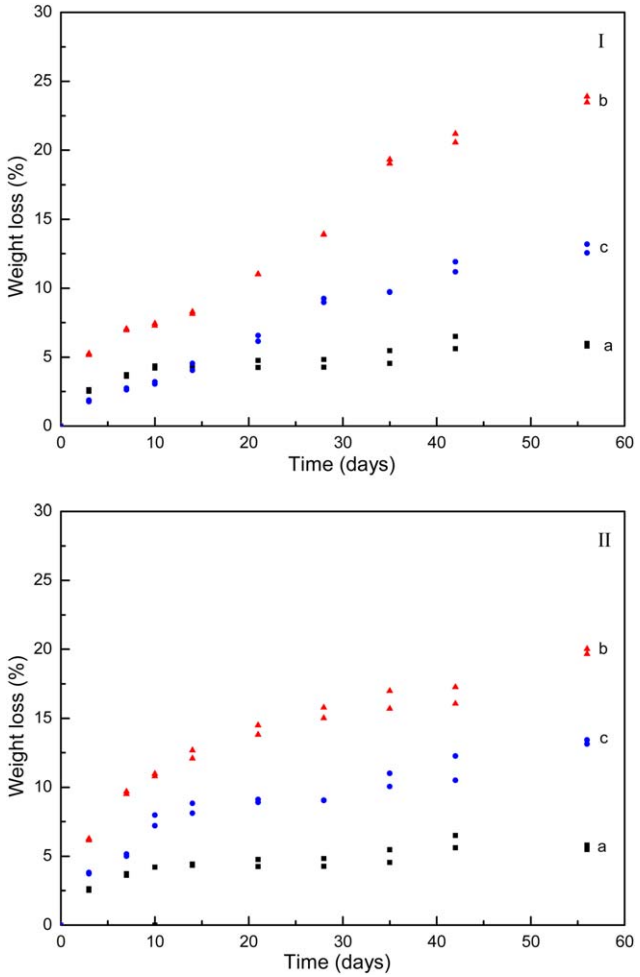

Figure 6. (I) Total weight loss (I) (it takes into account all soluble compounds: drug and PLA oligomers) and (II) polymer weight loss (weight loss due only to PLA oligomers) of: (a) neat PLA, (b) PLA/Bph and (c) PLA/LDH-Bph films. [Color figure can be viewed in the online issue, which is available at wileyonlinelibrary.com.]

the contact angle, thus, increasing the hydrophilicity of the sample. The presence of clay layers creates a labyrinth that affects oligomer diffusion and, therefore, retards degradation.[51] However, after approximately 14 days of hydrolysis, the weight loss of PLA/LDH-Bph surpasses that of pure PLA and after 56 days, the mass loss is around 12 wt %. This acceleration of mass loss was observed by Roy *et al.* in PLA/cationic clay nanocomposites and was explained by the catalytic effect produced by the oligomers whose diffusion is retarded by the presence of the clays.[36]

Table I. Water Contact Angles for the Different Films

Sample	Contact angle (degrees)
PLA	84
PLA/Bph	86
PLA/LDH-BPh	69

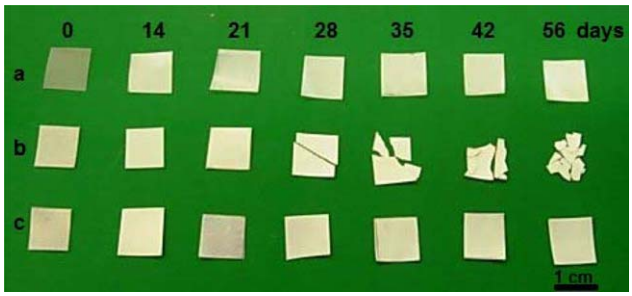

Figure 7. Visual aspect of (a) neat PLA, (b) PLA/Bph and (c) PLA/LDH-Bph after 0, 14, 22, 28, 35, 42 and 56 days under incubation in PBS (pH = 7.2) at 37 °C. [Color figure can be viewed in the online issue, which is available at wileyonlinelibrary.com.]

Visual images of PLA/LDH-Bph (Figure 7) show that the mass loss at 56 days is not enough to produce breakage and fragmentation of the films.

Thermal Properties

The effect of hydrolytic degradation on the crystallization of films exposed to the hydrolysis medium was further studied by DSC analysis. DSC scans corresponding to second heating for neat PLA, PLA/Bph and PLA/LDH-Bph degraded in buffer solution at 0, 14, 21, 35, 42 and 56 days are shown in Figure 8.

For neat PLA [Figure 8(a)] at 0 days the glass transition temperature (T_g) can be observed at 61 °C. A small decrease in T_g is observed as incubation time increases, as a consequenceof the reduction of molecular weight (Figure 9). The formation of PLA oligomers may also have a plasticizing effect. After 35 days an exothermic peak corresponding to cold crystallization appears (T_{cc}). The area of this peak increases with degradation time having a value of 15.4 J/g at 56 days. This is also a consequence of the faster diffusion of shorter polymer chains formed during hydrolytic degradation. Such lower molecular weight PLA chains can crystallize faster than the original neat PLA molecules.

After 21 days, Figure 8(a) shows the appearance of a melting peak at $T_m = 153.3$ °C. The melting enthalpy increases with degradation time (also as a consequence of cold crystallization which is evident from 35 days onwards) and the melting point remains approximately constant. The increase in the capability of PLA crystallization with degradation time is due to chain scission of ester bonds and to the consequently decrease in molecular weight. Two phenomena could be contributing to the possible increase in crystallinity with degradation time: crystallization or erosion of amorphous part. In order to elucidate which of these two effects is more important the treatment of Joziasse *et al.*[52] was used.

Joziasse *et al.*[52] consider that the mass of crystalline material at any degradation time t, $m_c(t)$, can be expressed as:

$$m_c(t) = X_c(t).m(t) = \left(\frac{\Delta H_f(t)}{\Delta H_f^0}\right).m(t) = \left(\frac{\Delta H_f(t)}{\Delta H_f^0}\right).m_0.[1 - m_1(t)] \quad (2)$$

where $X_c(t)$ is the crystallinity degree obtained from the first heating scans (Supporting Information Figure S1), $\Delta H_f(t)$ is the heat of fusion of the sample, ΔH_f^0 is the heat of fusion of

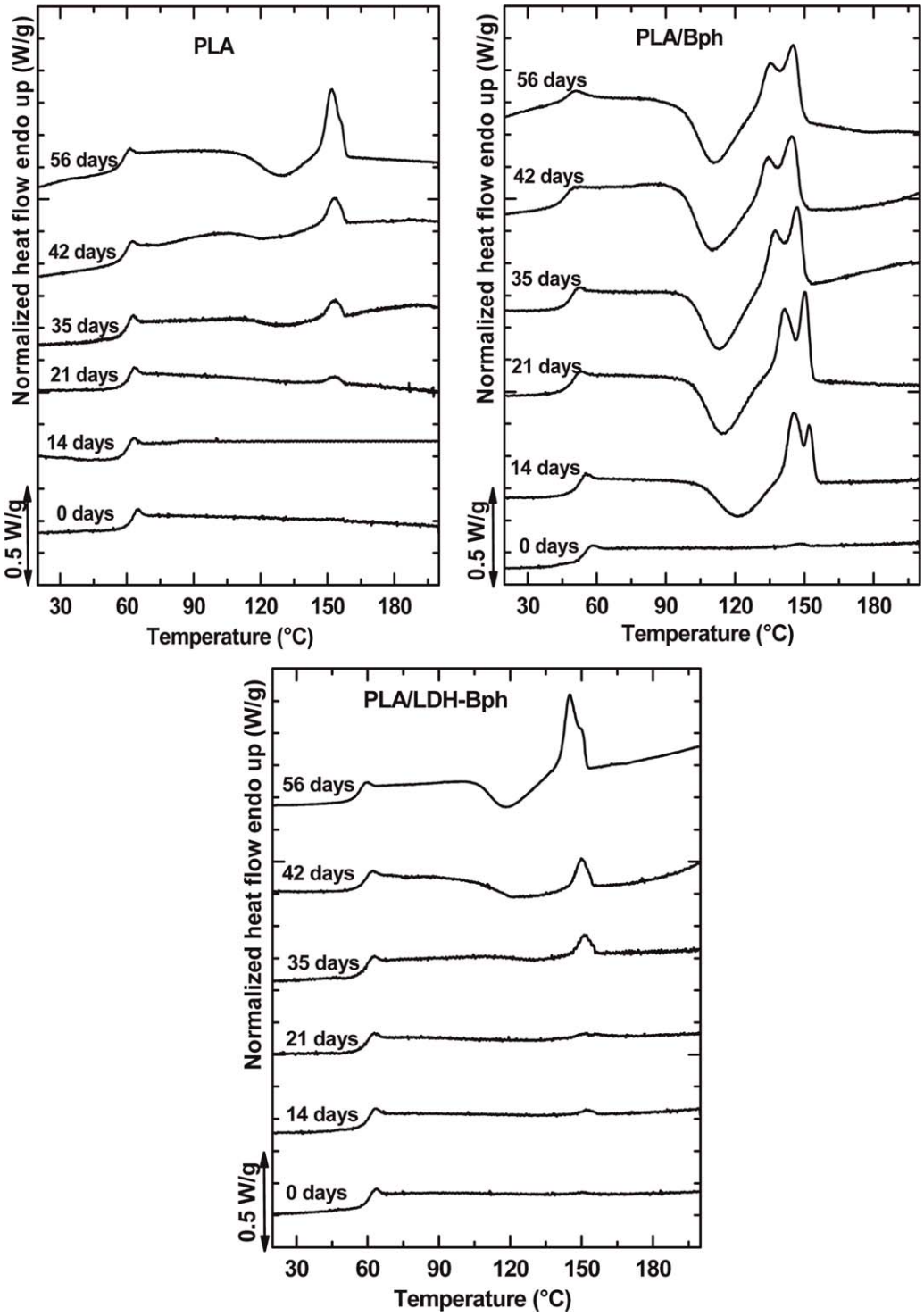

Figure 8. DSC second heating scans for PLA, PLA/Bph and PLA/LDH-Bph as a function of exposure time to the hydrolysis medium: (a) PLA, (b) PLA/Bph and (c) PLA/LDH-Bph.

the 100% crystalline material, m_0 is the initial mass, $m(t)$ the remaining polymer mass at time t, and $m_1(t)$ the polymer mass loss at time t [i.e., $m_1(t)=1-m(t)/m_0$].

The amount of crystalline material relative to the initial value $m_c(0)$ can be written as a function of time as:

$$\frac{m_c(t)}{m_c(0)}=\left(\frac{\Delta H_f(t)}{\Delta H_f(0)}\right).[1-m_1(t)] \quad (3)$$

where $\Delta H_f(0)$ is the heat of fusion of the original material.

Equation (3) allows the distinction between crystallization and degradation of the amorphous fraction. A constant $\frac{m_c(t)}{m_c(0)}$ with

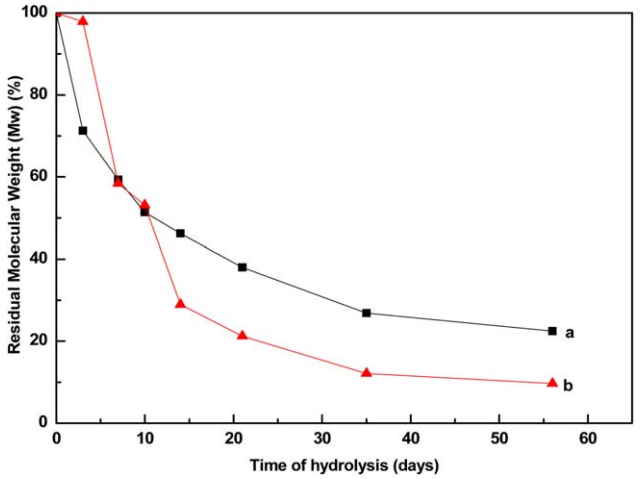

Figure 9. Time evolution of weight average molecular mass of (a) neat PLA and (b) PLA/Bph films, during hydrolysis in PBS (pH = 7.2 and 37 °C). No GPC measurements of PLA/LDH-Bph have been carried out because the filtration of samples does not ensure the total elimination of clay layers from samples. [Color figure can be viewed in the online issue, which is available at wileyonlinelibrary.com.]

time indicates that only the amorphous fraction degrades. An increasing $\frac{m_c(t)}{m_c(0)}$ points to crystallization of the amorphous phase, but if $\frac{m_c(t)}{m_c(0)}$ decreases, the crystalline material hydrolyzes.

A representation of eq. (3) is shown in Figure 9. It can be observed that for neat PLA $\frac{m_c(t)}{m_c(0)}$ initially increases with time and after several days it reaches a constant value, pointing to the degradation of the amorphous phase, according to the model of Joziasse *et al.* [52]

In the case of drug-loaded PLA (PLA/Bph) the T_g is lower than for neat PLA as a consequence of the plasticizing effect of Bph. Cold crystallization appears at 14 days, that is, earlier as compared to neat PLA. T_{cc} is lower than in the case of neat PLA and it decreases when degradation time increases. On the other hand the enthalpy of crystallization increases. Both results are consequence of the molecular weight reduction (Figure 9) that produces shorter polymer chains that crystallize easier. In Figure 10, it can be observed that initially $\frac{m_c(t)}{m_c(0)}$ increases with time but after 14 days it reaches a constant value indicating a degradation of amorphous part. These DSC results show that hydrolytic degradation is enhanced in the presence of the acidic drug leading to a higher decrease in molecular weight and consequently, to a higher crystallization.

At 14 days of incubation, drug-loaded PLA (PLA/Bph) exhibits two melting peaks, the first peak, corresponding to melting of the lamellae initially present in the sample. It decreases from 145 °C to 135 °C with degradation time. The second peak that corresponds to reorganization/recrystallization during the heating scan, decreases from 152 °C to 145 °C.

In the case of PLA/LDH-Bph T_{cc} is lower than for neat PLA and a melting peak can be observed as earlier as 14 days. These results suggest that the presence of drug incorporated to LDH

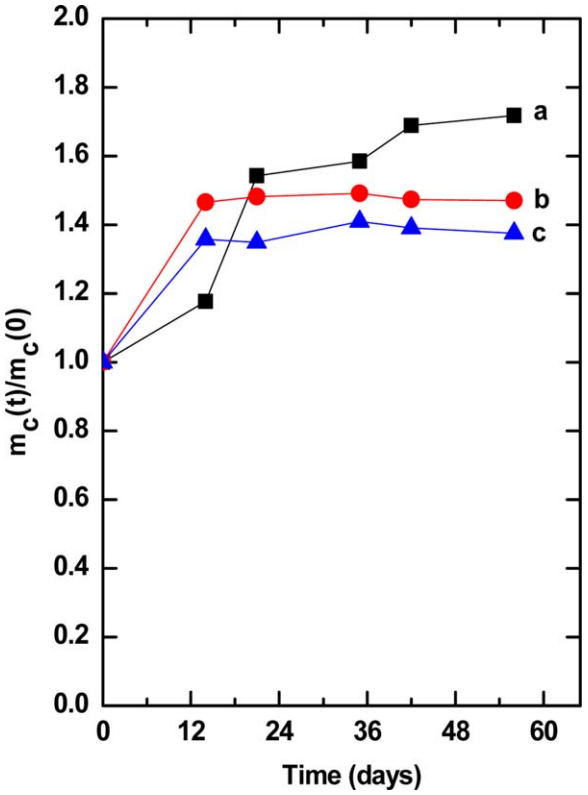

Figure 10. Variation of relative crystalline fraction [eq. (3)] as a function of hydrolysis time of (a) PLA, (b) PLA/Bph and (c) PLA/LDH-Bph. [Color figure can be viewed in the online issue, which is available at wileyonlinelibrary.com.]

affects PLA crystallization. However, as the drug amount is lower than in PLA/Bph (1.2 wt % in PLA/LDH-Bph compared to 5 wt % in PLA/Bph) this effect is moderate.

Surface Properties

SEM surface micrographs of neat PLA, PLA/Bph and PLA/LDH-Bph at 0, 28 and 56 days of degradation are shown in Figure 11. Prior to degradation (0 days) all films show a smooth surface. At 28 and 56 days, the neat PLA film surfaces [Figure 11(b,c) appear relatively smooth but with a porous structure as consequence of the degradation of the amorphous regions. At 56 days [Figure 11(c)] a slight increase in size and width of pores is observed.

For PLA/Bph film at 28 days [Figure 11(b′)] the surface is rougher than for neat PLA and with some debris. At 56 days [Figure 11(c′)] an increase in size and width of the pores is observed.

For PLA/LDH-Bph at 28 days [Figure 11(b″)] the distribution of pores is more heterogeneous than for neat PLA or PLA/Bph. This suggests that for the nanocomposites the degradation starts at the surface of LDH layers.

CONCLUSIONS

LDH has been modified with the drug 4-biphenyl acetic acid and the modification has been proved successfully using XRD and FTIR.

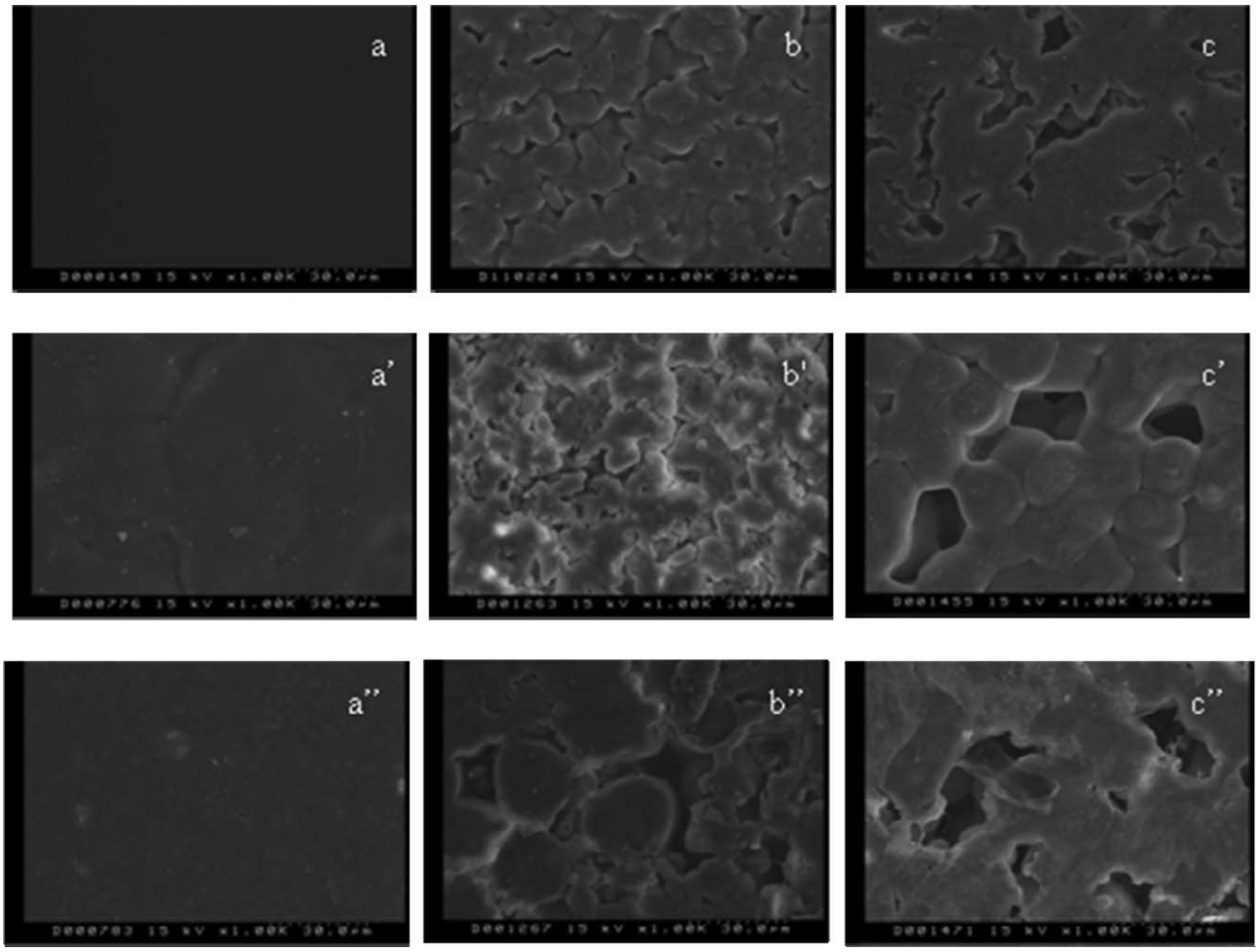

Figure 11. SEM surface micrographs of samples after different degradation times in PBS (pH = 7.2) at 37 °C: (a,b,c) neat PLA after 0, 28 and 56 days, respectively. (a′,b′,c′) PLA/Bph after 0, 28 and 56 days, respectively. (a″,b″,c″) PLA/LDH-Bph after 0, 28 and 56 days, respectively.

A nanocomposite of PLA and the drug-modified LDH has been prepared by solvent casting method (PLA/LDH-Bph). The obtained nanocomposite has a partially exfoliated morphology as determined by TEM.

The drug employed here accelerates the hydrolytic degradation of PLA matrix due to an acid catalytic effect. However, the presence of LDH produces a reduction of the initial mass loss compared to that of neat PLA, as a consequence of the barrier effect of LDH layers to the diffusion of the oligomers formed during PLA hydrolytic degradation. This retardation effect is followed by an acceleration that is a consequence of the catalytic effect produced by the oligomers, whose diffusion has been retarded by LDH.

The DSC results show that a higher crystallization is obtained in the case of PLA/Bph due to the higher decrease in molecular weight, as a consequence of the acid catalysis of the hydrolytic degradation that produces shorter polymeric chains. The time evolution of the amount of crystalline material relative to the initial value indicates that initially, the amorphous PLA phase crystallizes but after several days this amorphous phase starts to degrade. In PLA/LDH-Bph this effect is less acute because the amount of drug is lower.

The study of the film surfaces after the hydrolytic degradation show that for the nanocomposite, the degradation starts at the surface of the LDH thus producing a more heterogeneous distribution of pores than in PLA or PLA/Bph.

ACKNOWLEDGMENTS

Andrea Oyarzabal acknowledges the fellowship from the Basque Goverment. Financial support is acknowledged from UPV/EHU (UFI11/56), "UPV/EHU Infrastructure: INF 14/38"; "Mineco/FEDER: SINF 130I001726XV1/Ref: UNPV13–4E–1726" and "Mineco MAT2014-53437-C2-P" Technical and human support provided by SGIker is also acknowledged.

REFERENCES

1. Nair, L. S.; Laurencin, C. T. *Prog. Polym. Sci.* **2007**, *32*, 762.
2. Khang, G.; Rhee, J. M.; Jeong, J. K.; Lee, J. S.; Kim, M. S.; Cho, S. H.; Lee, H. B. *Macromol. Res.* **2002**, *11*, 207.
3. Ikada, Y.; Tsuji, H. *Macromol. Rapid. Commun.* **2000**, *21*, 117.

4. Zilberman, M.; Nelson, K. D.; Eberhart, R. C. *J. Biomed. Mater. Res. B* **2005**, *74*, 792.
5. Liu, H.; Zhang, J. *J. Polym. Sci. Polym. Phys.* **2011**, *49*, 1051.
6. Tsuji, H.; Tsuruno, T. *Polym. Degrad. Stabil.* **2010**, *95*, 477.
7. Lu, J.; Qiu, Z.; Yang, W. *Polymer* **2007**, *48*, 4196.
8. Ray, S. S.; Bousmina, M. *Prog. Mater. Sci.* **2005**, *50*, 962.
9. Pan, P. J.; Zhu, B.; Dong, T.; Inoue, Y. *J. Polym. Sci. Polym. Phys.* **2008**, *46*, 2222.
10. Ray, S. S.; Maiti, P.; Okamoto, M.; Yamada, K.; Ueda, K. *Macromolecules* **2002**, *35*, 3104.
11. Lyons, J. G.; Holehonnur, H.; Devine, D. M.; Kennedy, J. E.; Geever, L. M.; Clement, P. B.; Blakie, P.; Higginbotham, C. L. *Mater. Chem. Phys.* **2007**, *103*, 419.
12. Campbell, K.; Craig, D. Q.; McNally, T. *Int. J. Pharm.* **2008**, *363*, 126.
13. Campbell, K.; Qi, S.; Craig, D. Q.; McNally, T. *J. Pharm. Sci.* **2009**, *98*, 4831.
14. Leroux, F.; Aranda, P.; Besse, J. P.; Ruiz-Hitzky, E. *Eur. J. Inorg. Chem.* **2003**, 1242.
15. Costantino, U.; Marmottini, F.; Nocchetti, M.; Vivani, R. *Eur. J. Inorg. Chem.* **1998**, 1439.
16. Del Arco, M.; Fernández, A.; Martín, C.; Rives, V. *Appl. Clay Sci.* **2009**, *42*, 538.
17. San Román, M. S.; Holgado, M. J.; Salinas, B.; Rives, V. *Appl. Clay Sci.* **2012**, *55*, 158.
18. Hussein, M. Z.; Shazlirah, N.; Rahman, N. S. S.; Sarijo, S. H.; Zainal, Z. *Int. J. Mol. Sci.* **2012**, *13*, 7328.
19. Tammaro, L.; Constantino, U.; Nocchetti, M.; Vittoria, V. *Appl. Clay Sci.* **2009**, *43*, 350.
20. Tammaro, L.; Costantino, U.; Bolognese, A.; Sammartino, G.; Marenzi, G.; Calignano, A.; Teté, S.; Mastrangelo, F.; Califano, L.; Vittoria, V. *Int. J. Antimicrob. Agents* **2007**, *29*, 417.
21. Dagnon, K. F.; Ambadapadi, S.; Shaito, S.; Ogbomo, S. M.; DeLeon, V.; Golden, T. D.; Rahimi, M.; Nguyen, K.; Braterman, P. S.; D'Souz, N. A. *J. Appl. Polym. Sci.* **2009**, *113*, 1905.
22. Chakraborti, M.; Jackson, J. K.; Plackett, D.; Gilchrist, S. E.; Burt, H. M. J. *Mater. Sci. Mater. Med.* **2012**, *23*, 1705.
23. Miao, Y. E.; Zhu, H.; Chen, D.; Wang, R.; Tjiu, W. W.; Liu, T. *Mater. Chem. Phys.* **2012**, *15*, 623.
24. San Román, M. S.; Holgado, M. J.; Salinas, B.; Rives, V. *Appl. Clay Sci.* **2013**, *71*, 1.
25. Alexis, F. *Polym. Int.* **2005**, *54*, 6.
26. Grizzi, I.; Garreau, H.; Li, S.; Vert, M. *Biomaterials* **1995**, *16*, 305.
27. Vert, M.; Schwach, G.; Coudane, J. *J. Mater. Sci. Pure Appl. Chem.* **1995**, *32*, 787.
28. Nampoothiri, M. K.; Nair, N. R.; Hohn, R. P. *Bioresource Technol.* **2010**, *101*, 8493.
29. Frank, A.; Rath, S. K.; Venkatraman, S. S. *J. Control. Release* **2005**, *102*, 333.
30. Engineer, C.; Parikh, J.; Raval, A. *Trends Biomater. Artif. Org.* **2011**, *25*, 79.
31. Ray, S.; Yamada, K.; Okamoto, M.; Ueda, K. *Macromol. Mater. Eng.* **2003**, *88*, 58.
32. Paul, M. A.; Delcourt, C.; Alexandre, M.; Degé, P.; Monteverde, F.; Dubois, P. *Polym. Degrad. Stabil.* **2005**, *87*, 535.
33. Chen, H.; Chen, J.; Chen, J.; Yang, J.; Huang, T.; Zhang, N.; Wang, Y. *Polym. Degrad. Stabil.* **2012**, *97*, 2273.
34. Zhou, Q.; Xhantos, M. *Polym. Degrad. Stabil.* **2008**, *93*, 1450.
35. Fukushima, K.; Tabuani, D.; Dottori, M.; Armentano, I.; Kenny, J. M.; Camino, G. *Polym. Degrad. Stabil.* **2011**, *96*, 2120.
36. Roy, P. K.; Hakkarainen, M.; Albertsson, A. C. *Polym. Degrad. Stabil.* **2012**, *97*, 1254.
37. Chiang, M. F.; Wu, T. M. *Compos. Sci. Technol.* **2010**, *70*, 110.
38. Chiang, M. F.; Chu, M. Z.; Wu, T. M. *Polym. Degrad. Stabil.* **2011**, *96*, 60.
39. Zhou, Q.; Xanthos, M. *Polym. Eng. Sci.* **2010**, *50*, 320.
40. Castelli, F.; Pitarresi, G.; Tomarchio, V.; Giamona, G. *J. Control. Release* **1997**, *45*, 103.
41. Jmol. Available at: http://www.jmol.org, accessed December 10, **2015**.
42. Khan, A. I.; Lei, L.; Norquist, A. J.; O'Hare, D. *Chem. Commun.* **2011**, *22*, 2342.
43. Oriakhi, C. O.; Farr, I. V.; Lerner, M. M. *J. Mater. Chem.* **1996**, *6*, 103.
44. Kanezaki, E. *Mater. Res. Bull.* **1998**, *33*, 773.
45. Li, S.; Girod-Holland, S.; Vert, M. *J. Control. Release* **1996**, *40*, 41.
46. Tsuji, H.; Ikada, Y. *Polym. Degrad. Stab.* **2000**, *67*, 179.
47. Ma, Z. W.; Gao, C. Y.; Gong, Y. H.; Shen, J. C. *Biomaterials* **2003**, *24*, 3725.
48. Viera, A. C.; Vieira, J. C.; Ferra, J. M.; Magalhaes, F. D.; Guedes, R. M.; Marques, A. T. *J. Behav. Biomed.* **2011**, *4*, 451.
49. Agrawal, C. M.; Athanasiou, K. A. *J. Biomed. Mater. Res. A* **1997**, *38*, 105.
50. Verheyen, C. C. P. M.; De Wijn, J. R.; Van Blitterswijk, C. A.; De Groot, K. *J. Biomed. Mater. Res.* **1992**, *26*, 1277.
51. Yano, K.; Usuki, A.; Okada, A. *J. Polym. Sci. Polym. Chem.* **1997**, *35*, 2289.
52. Joziasse, C. A. P.; Grijpma, D. W.; Bergsma, J. E.; Cordewener, F. W.; Bos, R. R. M.; Pennings, A. J. *J. Colloid Polym. Sci.* **1998**, *276*, 968.